

## Compact Modelling of Electric Arc Furnace Electrodes for Vibration Analysis, Detection and Suppression

E. Brusa<sup>1</sup>, E. Franceschinis<sup>2</sup> and S. Morsut<sup>2</sup>

**Abstract:** Electrodes motion and positioning are critical issues of the Electric Arc Furnace (EAF) operation in steelmaking process. During the melting process electrode is exposed to some impulsive and harmonic forces, superimposing to the structure's static loading. Unfortunately, structural vibration may interact with the electric arc regulation, because of the dynamic resonance. Instability in the furnace power supplying and dangerous electrode breakage may occur as a consequence of those dynamic effects. In this paper the dynamic behaviour of a real EAF structure is discussed and some numerical models are proposed. Available experimental data, collected by a monitoring system on a real operating plant, allowed detecting the relevant phenomena related to the electrodes' vibration. Flexural and torsional modes were observed and so-called 'common' and 'differential' flexural modes were detected and distinguished, thanks to a deep numerical investigation. A full three-dimensional FEM analysis was performed to identify the global and local effects of vibration. Modelling activity was then aimed at shortening both the modelling and the computational times. Some approaches, based on different elements and mesh refinements, were then compared. Changes in the natural frequency of the structure due to the variable instantaneous position of the arm was tracked to suitably set a notch filter on the motion control. A further model order reduction was implemented to simplify the structural model. Experimental validation was preliminary performed on the existing plant and some confirmations on the effectiveness of the proposed models were found.

**Keywords:** Electric Arc Furnace (EAF), Vibration monitoring, Vibration suppression, Modal analysis, Finite Element Method, Model Order Reduction.

---

<sup>1</sup> Department of Mechanics, Politecnico di Torino, Italy; eugenio.brusa@polito.it

<sup>2</sup> R&D Division (CRD), Danieli SpA, Buttrio (Udine) Italy; s.morsut@danieli.it, e.franceschinis@danieli.it

## 1 Introduction

Electric Arc Furnace, usually referred to as “EAF”, is a primary metallurgical plant, designed to produce steel. Some typical aspects of this plant are described in [VDE, 1992]. It is currently widely used because of its flexibility in producing several grades of steel, although this kind of service needs a precise control and balance of the materials inside the furnace. Some analytical models of balancing techniques are already available and assure a quite good prediction of the actual performance of the furnace, as it was documented by [Chirattananon and Gao, 1996; Abraham and Chen, 2008]. This plant is currently considered strategic since it allows melting even ferrous scrap [Crompton, 2001], because both the hot metal and directly reduced iron may be used as charged materials. The energy required by the melting process is mainly delivered by electric arcs, directly striking to the charge or to the metallic bath. The productivity and energy consumption of the EAF depend on the overall regulation system, which suitably generates and controls the maximum availability of electric power at the charge. The energetic performance of the EAF system can be evaluated by simplified models as is in [Chirattananon and Gao, 1996]. Regulation is performed by continuously controlling the position of the graphite electrodes within the furnace, by lifting and lowering the heavy arms holding them (Figure 1).



Figure 1: Electrode regulation system for the three-phase alternate current arc furnace analyzed

The graphite electrodes are held by conductive arms, which have both the structural function and the goal of feeding the electric current to generate the arc (Figure 1). Very high currents, up to 90 kA, are fed through the arm. They motivate a special structural design of the arms. Copper clad steel plates are weld to create a shell and are internally cooled in operating conditions. Current flows through the outer

copper layer having a lower electrical resistivity, even helped by the skin effect. The internal structural steel plate is free from Joule heating, therefore it does not affect the EAF performance at all. Conductive arms are directly connected to the secondary of the EAF's transformer by long and flexible cables. The arm and the electrode are supported by a mast, which is kept vertical by a set of guiding rolls (Figure 1).

The mast includes a single-acting hydraulic cylinder, which allows the electrodes positioning. A high-speed digital regulator is used to control the arc voltage and current by upsetting the electrode position. It acts on a proportional valve which is connected to the hydraulic cylinder, inside the mast. The valve assures a fairly fast dynamic response. A sketch of the regulation and power supplying systems is shown in Figure 2.

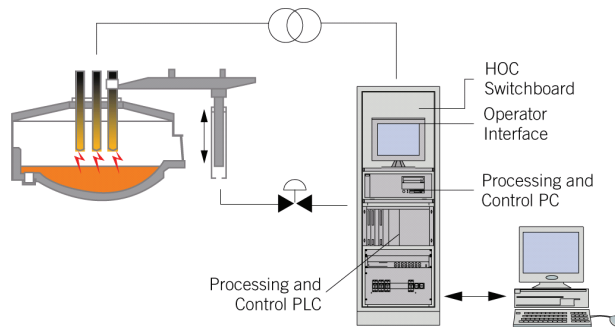


Figure 2: “Hi-reg” electric arc regulator scheme (courtesy of Danieli)

Electrodes, arm and mast constitute an elastic structure, weighting several tens of tons and affecting the electrical response to the control command. In the first step of the melting process the electrode may collide to the scrap, deposited inside the furnace. This collision may cause severe short-circuits, with high currents, thus requiring a very fast reaction to the regulator, which controls the electrode position. Some inertial loads are originated and they excite an uncontrolled oscillation of the structure, at its natural frequency. This vibration turns out in a potential instability of the electrical control variables, responsible of power supplying. Feedback compensation of the electrode regulator may interact with the system's natural frequencies generating a resonance, which sometimes breaks the electrode. These damages are observed in operating conditions and have to be predicted by the mechanical design [Franceschinis, 2007].

During the melting process frequencies at which EAF's structure vibrates are progressively lowering, because of the interaction with the regulation valve behaviour.

At a certain level they affect the active power supplying, thus causing a less efficient power consumption, an irregular radiation of heat due to the exposed arc and a decreasing of the structural strength of the electrodes. These effects are evident in the voltage and current time histories and motivate the application of an adaptive control technique able to compensate for the changes of the system parameters [El-Saady, 2001]. In the past industrial practice was mainly based on the direct monitoring and experimental measuring of these dynamic phenomena. Nowadays, modern plants need a modelling activity supporting the design and regulation operations. The very fast production required to this kind of furnace increased the amount of failures detected on the system, particularly in the transformer connected to the furnace and in the system components. This required to propose some strategies to prevent these failures, as it is documented by [Marsical and Martinez, 2008] and [Boyd and Sikka, 2008], for the two aspects above mentioned. Numerical modelling may help to achieve this target. A detail model of the whole system accurately predicts its dynamic behaviour. Moreover, it shall allow scaling suitably this technical problem to design a new generation of EAF, whose sizes are fairly different from the plants currently available. This goal is followed in this work and a structural analysis of the system is performed. In particular, dynamic phenomena are detected on an operating EAF and modelled by means of the Finite Element Method (FEM). Numerical models are experimentally validated. A perspective of control is finally given and tested. Two goals are simultaneously achieved in this research activity. A first result consists in providing the designer a compact structural model to be used in some analysis of the system performance. A second feature corresponds to the interpretation of some problems monitored either in the structural or electrical part of the EAF system, which are related to some specific resonances of the structure and the corresponding mode shapes.

## **2 EAF performance and modeling requirements**

A screening on the existing technical literature about the design and operation of the EAF reveals that a key feature in the performance evaluation are the mass and energy balances. A precise computation of the energy supplied to the scrap and to the bath in the steelmaking operation is required to predict the amount and the grade of the steel produced as well as the electric power required. Therefore, technical contributions were mainly focused on some typical aspects herewith shortly mentioned. Some analytical models of mass and energy balance within the furnace are developed and improved over time, up to the most recent techniques proposed by [Abraham and Chen, 2008], and currently tested on operating plants like in [Ekmecki et al., 2007]. Process and cooling system control are continuously improved, even by resorting to the robust control strategies, to manage the fast changes in the

system parameters [Shinohara and Goodall, 2004]. Finally, power generation and control is a key issue of the research from both the points of view of the performance evaluation and the system regulation as it is deeply described by [Camdali et al., 2003; El-Saady, 2001]. To deal with the above mentioned issues of the EAF design, several models were developed. They are basically analytical and consist of simplified balance equations, able to give an overall performance evaluation of the plant, but practically unsuitable for a detailed design of subsystems, including the mechanical structures, the electrical system and the ferrous scrap. To cope with this lack of information some recent contributions dealt with those details of the EAF's operation, previously neglected or insufficiently modelled. A first one is the thermoelectric coupling in the EAF system responsible of some inefficient predictions of the transient behaviour of electrodes. Numerical models were applied to investigate the behaviour of the electric field around the electrodes and its interaction with temperature [Bermudez et al., 2003]. A second example concerns the scrap motion inside the furnace, which affects preheating operation and melting process. A preliminary model was proposed by [Guo, 2007]. Both the above mentioned effects were indirectly detected since several years as source of supply-voltage fluctuation, but never modelled, because of the difficulty associated to the prediction of coupled system dynamics and in modelling inhomogeneous materials [Dixon, 1972]. Surprisingly, no contribution in the literature systematically dealt with the structural dynamic behaviour of the electrodes and of supporting arms. Vibration is responsible of some failures, occurring equally as structural damage and as irregularity in power supplying and arc generation according to [Marsical and Martinez, 2008; Bermudez et al., 2003]. This task is performed herewith, by studying the mechanical behaviour of the EAF structures and comparing numerical results to the evidences of an experimental vibration monitoring operated on an operating plant.

### **3 Numerical approach**

Industrial practice and technical standards motivated applying numerical methods to perform the dynamic analysis of the EAF structure. The FEM was preferred, being recognized to be a suitable tool to perform the structural analysis of these industrial components. Models are here used to accurately predict the structural dynamics as well as to design an electrode regulation system including a reduced order model of the structural components. EAF structures were modelled by resorting to both beam and solid/shell elements. This comparison allowed investigating the level of accuracy achieved by the available finite elements.

Evaluating the stiffness and the inertia of all the components of the EAF mechanical assembly looks crucial to build an effective model. The operational flexibility

of the beam element is suitable to easily evaluate these aspects and to point out weak and over-sized parts of the structure. Nevertheless, a model based on beam elements demonstrated to be insufficient to describe the actual response of this system [Franceschinis, 2007]. A full three dimensional model, including solid and shell elements, is more expensive in terms of computational time, but assures a good prediction of the actual dynamic behaviour of the EAF. As it shall be deeply documented later, a model including beam elements describing arm, mast and electrodes, and solid and shell elements, used for the connecting parts only, looked to be suitable enough to fit the experimental evidences and to decrease the modelling and computational times.

Vibration mode shapes occurring at the lowest frequency were studied to identify the actual origin of the detected resonance among the hydraulic actuator excitation, the structure and other sources. This investigation allowed defining suitable criteria for the design activity. In particular, while structural resonance is avoided by stiffening some mechanical components, hydraulic actuator may be controlled by applying a narrow band notch filter to the valve action. Band notch filtering is a known approach proposed for a simple vibration suppression [Meirovitch, 1999].

To improve the fastness of the design activity, model order reduction techniques have been implemented, after a preliminary validation of the numerical models, made possible by some experimental audits. Model order reduction was based on both the techniques proposed by Guyan [Guyan, 1965] and Craig-Bambpton [Craig and Bambpton, 1968] respectively. Although the first one is today widely implemented in FEM commercial codes, rigid body motion present in the furnace operation suggested to implement the Component Mode Synthesis (CMS) developed by Craig and Bambpton. Therefore, a preliminary run of FEM code ANSYS® was used to identify master degrees of freedom and mode shapes to be retained into the reduced model. Numerical results were compared to the experiments performed during the maintenance audits on the monitored EAF. Actually, this experimental activity appeared incomplete, because the number and location of the measurement points were selected only for maintenance purposes, never for a complete modal testing, as it is usually done in a laboratory, like Ewins deeply describes in [Ewins, 2000]. Nevertheless, the collected information was sufficient to validate the numerical models and the reduction techniques. The reduced model was then written in state-space formulation, to be included into the numerical simulator used to design the control system.

#### **4 Maintenance audits on the test case**

The steel plant of Sovel S.A., located in Volos (Greece), was selected as study case. This plant is described in detail in [Bouganopoulos et al., 2008]. This 80 MVA

AC-EAF, supplied by Danieli & C. Officine Meccaniche in the year 2000, produces 127 mt/h of steel. An experimental testing was performed during a normal maintenance shutdown period. Eight piezoelectric accelerometers Bruel&Kjaer Vibro AS-070/001, with measurement range spanning from 0.1 Hz to 10 kHz, were fastened on the conductive arm and on the mast (Figure 3). Acceleration was measured and signals recorded by a high-speed acquisition system based on National Instruments SCXI 1531 conditioning module and National Instruments DAQ 6062E acquisition card.

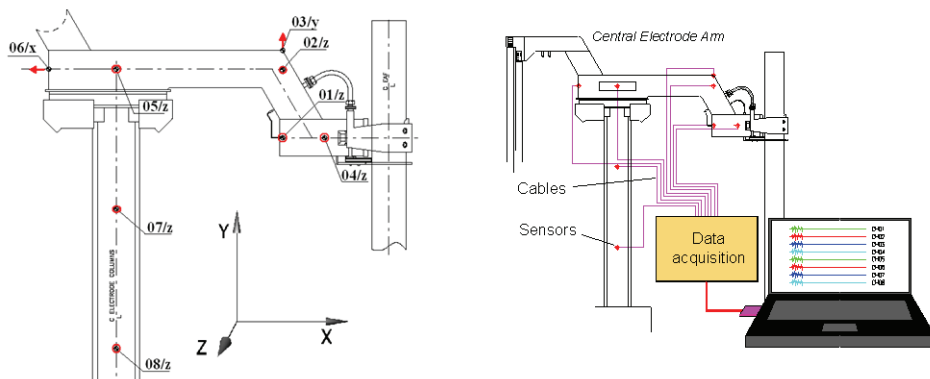


Figure 3: Experimental set-up available at the customer and used in maintenance audits.

To assure both the good excitation of the natural vibration of the EAF's structures and the safety of the operators, the instrumented hammer looked to be unsuitable, because of the system's size and the brittleness of the graphite electrodes. Therefore structural vibration was excited directly by means of the positioning system, as it actually occurs in operating conditions. Lifting and rotational motions of the structure were suddenly stopped, in correspondence of four values of the electrode elevation. A vertical impulse along the mast column was given by stopping the lifting motion of the regulation cylinder. This induced the electrode vibration depicted in Figure 4 (lateral view). Few tests were performed by stopping both the lowering and the raising mast motion. The lateral and torsional vibrations were excited by stopping the rotation about the vertical axis. This rotation is commonly used to swing the furnace roof before the charging of the ferrous scrap (Figure 4, top view).

Constraints acting on the structure were applied through the framework which connect the three electrode arms and the regulation system. According to the inspection

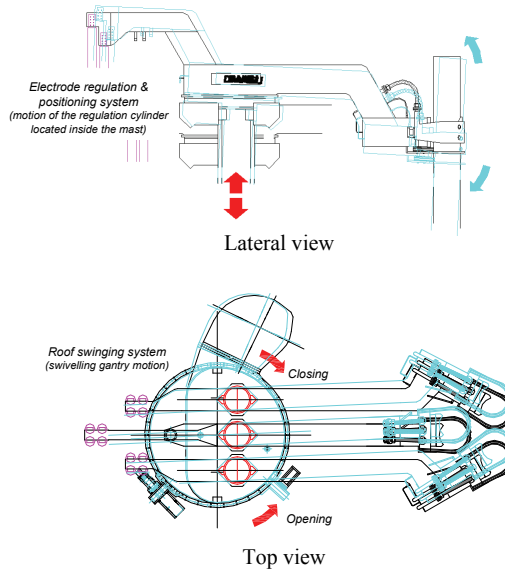


Figure 4: Excitations induced by the customer's team on the EAF structures during maintenance audits

protocol, some impulses are applied by suddenly locking the cylinder valve. No additional motion is possible at the connection to the structure if suitable constraints are applied to displacement and rotation.

Sensors location was selected by the customer, who has in charge the EAF maintenance. Unfortunately, these locations are only partially suitable to reconstruct the vibration modes of the structure. Each accelerometer detects the motion along a single direction described by the first number in Figure 3. In practice, the lateral motion of the clamping device, which supports the electrode, is described by sensors 01, 02 and 04, while its vertical motion is detected by 03. The mast lateral motion is monitored by sensors 05, 07 and 08. Accelerometer 03 detects the horizontal motion of the conductive arm. The rigid motion of the connection between the column and the arm was unfortunately very poorly monitored. Since excitation was applied without an instrumented device, each input signal corresponding to a motion stop was reconstructed by means of sensors 02, 03, 05 and 06.

## 5 Experimental results

Monitoring performed on the EAF provided thirteen dynamic tests. Each one recorded the accelerations measured by the eight transducers. Tests differ because

of the mast elevation and the impulse given either on lifting or rotational motion, as it is resumed in Table 1.

Table 1: Experimental tests performed during the maintenance audit

N.	Elevation [% max]	Force	Direction	Active accelerometers
1	Max	Lift up	down-up	All
2	Max	Lift up	down-up	All
3	Max	Lift up	down-up	All
4	Max	Lift up	down-up	All
5	Max	Lift up	up-down	All
6	90%	Lift up	down-up	All
7	90%	Lift up	down-up	All
8	78%	Lift up	down-up	All
9	72%	Lift up	down-up	All
10	Max	Rotation	opening	no 04z and 08z
11	Max	Rotation	opening	no 04z and 08z
12	Max	Rotation	opening	no 04z and 08z
13	Max	Rotation	closing	no 04z and 08z

A poor dynamic response was monitored in case of tests 2,4 and 5, while a significant amplitude in vibration was detected by transducers 03 e 06 in tests 3,6,8, 9 and by transducers 02 e 05 in case of tests 10 and 13. Therefore 3,6,8, 9, 10 and 13 tests were selected for the following analysis. In addition test 5 was included, being the unique complete measurement provided, obtained by stopping the arm during the lifting manoeuvre.

All the measured data were analysed in frequency domain, by means of the Fast Fourier Transform (FFT) according to the practice [Inman, 2008]. The complete time history of the acquired signal was elaborated. It included the preliminary transient response of the structure, shown in the very early part of the monitored vibration. This action allowed keeping the complete modal information used to characterize large flexible structures, like those studied by [Jenkins, 1993]. To perform a faster analysis was even applied a numerical sampling on the collected measures. Hanning window filter was applied by the operator to avoid the leakage phenomenon, as suggested by vibration control textbooks like [Inman, 2008; Franklin and Powell, 1990]. Signal processing was performed by means of MATLAB subroutines developed by the authors and some available toolboxes. Amplitude and phase of the dynamic response were computed to perform a modal analysis, as complete as the location and the number of transducers did allow. All the

experimental results are documented in the following sections and compared to the numerical results, computed by the FEM.

## 6 Numerical modeling through FEM

A full solid model of the structure and of the electrode regulation system was built (Figure 5). It was compared to a simpler model including beam elements. In case of the shell/solid elements a very refined mesh was applied. It included up to 45000 elements and 32000 nodes. This model definitely satisfies the standard requirement about the availability of an accurate numerical discretization of the whole system, as well as Bermudez et al. discussed in [Bermudez et al., 2003]. Nevertheless, it is really unsuitable to run a fast computation of the vibration modes and for the validation purposes. Moreover, the geometrical complexity of the structure required a number of simplifications to handle both the pre-processing and solution operations.

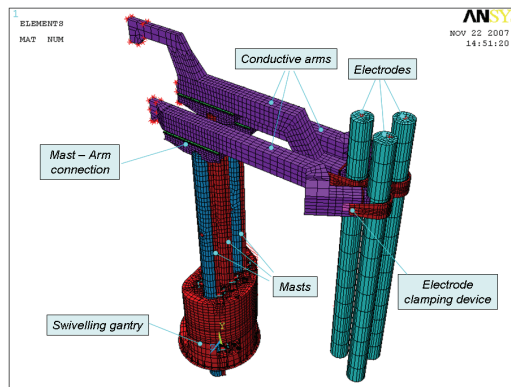


Figure 5: FE model based on Solid/Shell elements of the complete electrode regulation system

The furnace structures consists of three electrodes, three supporting arms and the elevating system composed by columns, connections and common gantry. Electrodes correspond to the three electrical phases. Therefore they are designed to be strictly independent. Since only the common gantry applies the constraints to all the masts with their arms and electrodes, vibration is practically uncoupled between the central phase electrode and the lateral ones. This assumption allows considering, at least preliminarily, that vibration of each set of mast, arm and electrode be isolated from the whole assembly. Since lateral phase electrodes are symmetric,

only two structures had to be modelled, i.e. the central and the lateral electrode respectively. Structural stiffness is very different among the components of this assembly. Sub-structuring operation was applied to analyse components with different compliance. Mast and electrodes exhibit a comparable compliance, while the common gantry is widely stiffer. Structure of the central electrical phase was analysed as first, then the lateral phase frame was modelled. These two sub-models included each one about 12000 nodes and 7000 elements.

Several were the crucial aspects of the modelling activity. A precise estimation of the inertial effect of the cables looks important to avoid a mistuning of the computed frequencies when they are compared to the experiments. This aspect was carried out by applying a massive and lumped parameters element to the end of the arm, according to [Genta, 1999]. This element simulated the portion of the cable mass towed by the structure in manoeuvring. According to industrial practice and to some references this mass was estimated to be approximately as an half the cable weight, like VDE Standards suppose in [VDE, 1992] and El-Saady in [El-Saady, 2001].

Another critical input in modelling consisted in representing the real constraint applied by the positioning system to the vertical mast. Each column is lifted up and lowered by means of eight wheels, which are in contact with the external profile of the mast (Figure 6). Contact is regressive, i.e. it is only assured by a bias force pushing the wheel on the moving column. In case of insufficient action the contact pressure vanishes. In principle this introduces a nonlinear action. Contact elements were preliminary introduced to take care of this aspect. In practice, it was observed that the bias force provided during the assembling of the guiding rolls could be sufficient to assure a permanent contact, without regression. This assumption allowed realizing, after few attempts, that it is sufficient to impose null displacements along x and z directions to nodes referred to as 1 and 4 in Figure 6. Rotational constraint was imposed as combination of null displacement to a couple of nodes, opposite in the column transversal section, to allow the detection of some torsional vibration modes (nodes referred to as 2 and 3 in Figure 6). This scheme was effective to simulate the real constraints and to avoid the transient dynamic analysis of the contact between guiding roll and vertical column. This approach was compared to the information and the models proposed by Wriggers in [Wriggers, 2006].

To replicate in FEM analysis the stopping action given to the elevation motion in experimental tests for each configuration a constraint to the vertical displacement, i.e. along y axis, was imposed on node referred to as 5 (Figure 6). It can be noticed that the connection between arm and electrode is provided by an elastic joint. It is stiffened during clamping manoeuvre to apply the required friction force and keep

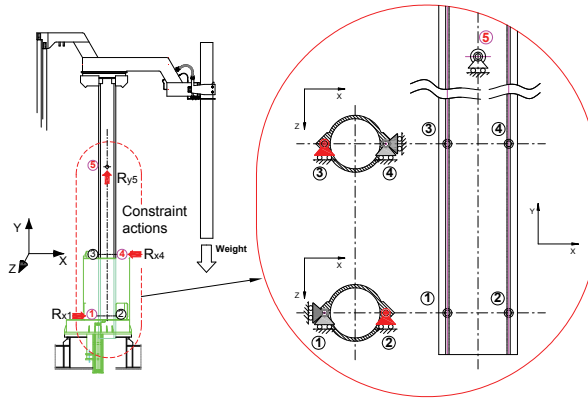


Figure 6: Constraints applied to the electrode lifting structure

the electrode in the desired position. This clamp was modelled by a stiff compliant constraint, available in the FEM code [ANSYS,2008].

Temperature is a relevant design parameter. The electrode is exposed to a huge increase of temperature, particularly at the beginning of the furnace operation. Nevertheless, the region most affected looks the lower end of the electrode, close to the scrap or to the metallic bath. This part is less significant from the point of view of vibration modes than the head and the connection to the arm. Moreover, a cooling system assures a quite stable temperature, within the range  $150 - 250$  °C, at which mechanical loads are applied to the electrode. Graphite's Young modulus increases with increasing temperature, as 1.3 MPa per degree Celsius. All the above mentioned remarks allow considering the test at room temperature the most relevant in terms of the mutual interference between the control system and the structure's dynamics. This assumption is conservative, at least for the lowest frequencies, at which the most dangerous vibration modes are excited. It is comparable to the hypotheses imposed by Sandberg [Sandberg et al., 2007], to model the scrap motion, and by Marsical and Martinez [Marsical and Martinez, 2008] dealing with the failure prevention of the electric circuit and devices, or by Shinohara and Goodall [Shinohara and Goodall, 2004] in setting the robust control system. A modal analysis was therefore performed at the room temperature, as it occurred during the experimental tests.

## 7 Numerical results and model assessment

The dynamic analysis of the central and lateral arms were carried out under the above mentioned assumptions. Since structures are conductive, they are composed

by layers of different materials. FEM implementation included: Steel ( $E=2.06 \cdot 10^{11}$  Pa,  $\nu=0.29$ ,  $\rho=7850 \text{ kgm}^3$ ), Copper ( $E=1.10 \cdot 10^{11}$  Pa,  $\nu=0.34$ ,  $\rho=8900 \text{ kgm}^3$ ), electrical insulator ( $E=2.0 \cdot 10^{10}$  MPa,  $\nu=0.4$ ,  $\rho=1850 \text{ kgm}^3$ ) and graphite ( $E=9.0 \cdot 10^9$  Pa,  $\nu=0.4$ ,  $\rho=1700 \text{ kgm}^3$ ). Models were developed in ANSYS®vs.10.0. They included 3883 Shell and 2204 Brick elements, 12322 nodes in the case of the analysis of the central phase electrode, 6413 Shell and 3477 Brick elements, 11578 nodes in the solution for the lateral phase electrode.

Table 2: Vibration mode shapes and frequencies of the central phase structure computed by ANSYS®[Hz]

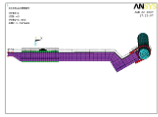
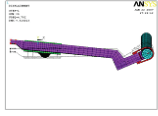
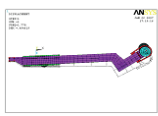
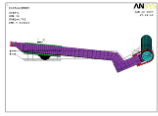
MODE SHAPE			COLUMN ELEVATION [mm]			
			500	2800	4500	5100
A		Column lateral bending and torsion	2.2409	2.0676	1.8727	1.7779
B		Complete bending ("pitching")	2.5667	2.4399	2.2951	2.2156
C		Electrode bending and slight column torsion	4.1090	3.0787	2.5422	2.4019
D		Electrode bending	4.2461	3.6046	3.1256	2.9806
E		Electrode and column bending, column torsion	13.101	6.5563	5.0305	4.7017
F		Column, arm, electrode bending	14.716	8.5737	6.6773	6.2772

Table 2 and 3 describe the first six mode shapes of the EAF structure and its dependence on the elevation of the conductive arm during the melting process. The natural frequencies of the depicted modes span from 1.5 Hz to 15 Hz. Relevant motions are due to vibration of the column, the arm and the electrode. Flexural

Table 3: Vibration mode shapes and frequencies of the lateral phase structure computed by ANSYS®[Hz]

MODE SHAPE			COLUMN ELEVATION [mm]			
			500	2800	4500	5100
A		Column lateral bending and torsion	2.2409	2.0676	1.8727	1.7779
B		Complete bending ("pitching")	2.5667	2.4399	2.2951	2.2156
C		Electrode bending and slight column torsion	4.1090	3.0787	2.5422	2.4019
D		Electrode bending	4.2461	3.6046	3.1256	2.9806
E		Electrode and column bending, column torsion	13.101	6.5563	5.0305	4.7017
F		Column, arm, electrode bending	14.716	8.5737	6.6773	6.2772

and torsional mode shapes are mainly excited. Several combinations of these two dynamic behaviours are exhibited (Figure 7).

Mode referred to as "A" in following Table 2 and 3 exhibits mainly a torsion of the column associated to a slight bending and to a more evident flexural response of the electrode. In mode called "E" the torsion is larger and still superimposed to the bending of the electrode. Some remarks can be drawn about this first observation. The existing literature is prone to assume that the main vibration involves the flexural behaviour of the electrode. This appears in the studies concerning both the arc regulation and the scrap motion [Bermudez, 2003; Guo, 2007]. A two dimensional model of such a mode shape is consequently used. Analysis pointed out that arm has a relevant contribution in mode shapes and torsional behaviour is even excited.

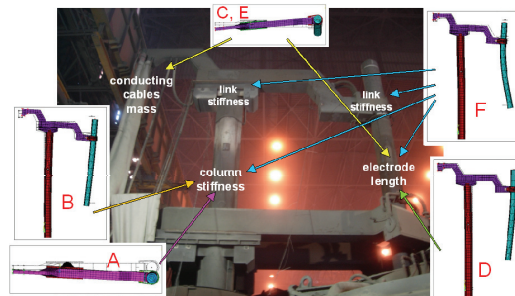


Figure 7: FEM analysis: description of the main mode shapes related to the structural components of the EAF system

A preliminary validation was performed by comparing the numerical and experimental results. It should be based on the comparison of both the mode shape and the detected values of the natural frequencies of the structure. Unfortunately, the experimental set-up available and the limited number of accelerometers did not allow a systematic recognition of the whole set of calculated mode shapes. Therefore a first validation was based on the detected experimental frequencies. Modes A, B and F were mostly considered, since they were mainly excited in testing. The calculated dynamic response of the central phase structure was found in good agreement with the data collected (Figure 8). It can be noticed that only a part of the available length range was investigated by the operators during the maintenance audit. Actually, authors were not allowed to access to the plant to modify this set-up, at least in this first run, because of safety reasons. Nevertheless, a second experimental campaign is currently foreseen to complete the above mentioned validation.

The same numerical investigation was performed on the lateral phase structure and on the full system, including the two lateral and the central electrodes. This analysis on the complete structure actually added a significant information. It allowed distinguishing some modes, in which electrodes vibrate in phase, from those characterized by a sort of out-of-phase oscillation. In the first case literature suggests the term “common mode vibration” to indicate that all the structures move in the same direction while vibrating [Junkins and Kim, 1993]. “Differential mode” is called the vibration in which two structural elements of the same system move in two opposite directions. The latter configuration strongly affects the arc generation and may cause severe problems in power control as it was observed in [Camdali, 2003; Marsical and Martinez, 2008], although it was not yet related to structural vibration.

The dynamic behaviour of the lateral phase electrode exhibited a set of natural fre-

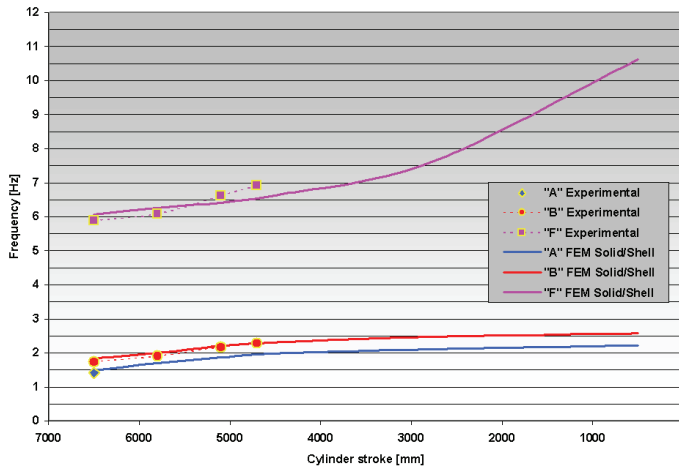


Figure 8: FEM analysis on the central phase electrode: validation of the numerical model by means of the experimental results

quencies fairly close to those of the central one and very similar mode shapes. A sort of map of influence on vibration mode shapes of the main structural components was drawn. Result is summarized in Figure 7.

Column structural stiffness significantly affects modes A, B and F. In case B and F a flexural behaviour of the column couples with the response of the supported electrode, while in mode A torsion of the column is strictly depending on its stiffness. Inertia of cables is important to predict precisely modes C and E, since they show a relevant motion of the arm. Compliance of the connection between arm, column and electrode affects mainly mode F, while the length of the electrode is dominant in mode D and partially in F.

The above analysis pointed out some remarkable aspects about modelling activity. Shell elements describe appropriately the dynamic behaviour of the investigated test case if the mesh is very fine as in the performed analysis. Sensitivity shown by the FEM model is very high, particularly concerning the modelling of the connection between arm and electrode, because of the assumptions made about the clamping system. The role of the constraints applied by the positioning system is crucial for a good agreement with the experimental results. These aspects have to be carefully considered in reducing the order of the FEM models. To properly model the mechanism of actuation and positioning applied to the vertical column, suitable number and location of master degrees of freedom in that part of the structure have to be included [Genta, 1999]. The proposed model assumes that vibration of the

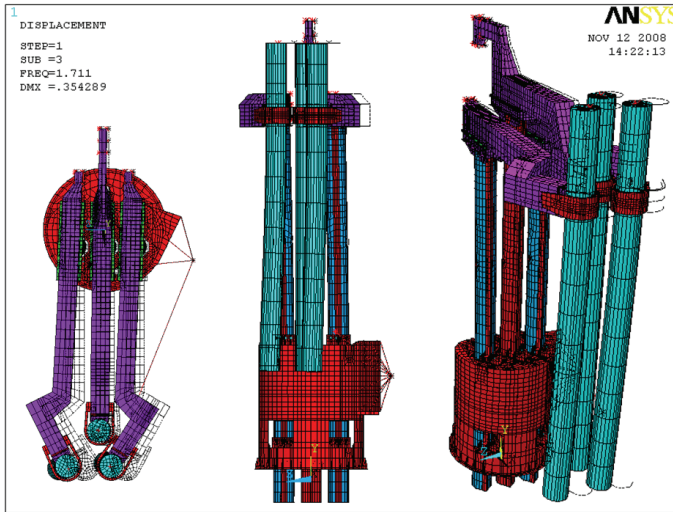


Figure 9: Full FEM model: transversal motion of the central phase arm excited by the lateral phase electrodes

central and lateral electrodes is uncoupled. It is effective in predicting the most significant mode shapes experimentally monitored. Nevertheless, few secondary coupling effects do exist and the complete description of the dynamic behaviour of the system is given only by the full model of the whole structure. Actually the transversal bending effect detected in the maintenance audit on the central electrode (at 1.7 Hz) was excited by the vibration of the lateral arms, as depicted in Figure 9. Torsional modes were poorly excited by the impulsive testing performed through the swivelling gantry.

## 8 Discussion and preliminary design improvement

The first mode shapes of the structure of the EAF occurring at the lowest values of frequency appear the most dangerous from the structural point of view. Differential mode shapes among the three electrodes are critical for the electric circuitry in terms of power consumption and arc generation. Common modes shapes of the electrodes strongly affect the scrap motion within the furnace (Figure 9). The electrode structure seen as a stand alone system has a first resonance approximately at 4 Hz, although the regulation command bandwidth spans from 2 to 10 Hz. A superposition between the structural resonance of the electrode and the typical frequency bandwidth of the motion control exists. Yaw motion of the conductive arm is quite

evident in operating condition. It is excited by the repulsive forces acting among the electrodes and superimposes to the fast lifting motion operated by the system regulation. A coupling between torsional and flexural behaviours is observed particularly in mode shape A, being extremely dangerous. This behaviour suggests a design improvement aimed at increasing this eigenfrequency and reducing the dynamic response to this impulsive force. An increasing of the torsional stiffness of the mast is currently performed by the designers. A reinforcement of the guiding rolls' reaction capacity is evenly completed.

An additional critical frequency is related to the electrode pitching mode B. This is dominated by the flexural stiffness respectively of the mast, the arm and of their mutual connection. Interaction between the regulation frequency and that of the pitching motion may result in a resonance phenomenon.

A first intervention foreseen by the operator to prevent the resonance consisted in avoiding the excitation of the structural natural frequencies by regulating the valve action on the hydraulic actuator. An immediate and economical strategy implemented on the plant was accomplished by imposing a notch filter control to the regulation command [Franklin et al., 1990]. It is aimed at cutting off all the command inputs sent to the valves, tuned on a frequency enclosed in the narrow bandwidth across the resonance value (Figure 10).

This tuning operation is rather difficult since the frequency of the pitching motion depends on the mast elongation. Higher elevations of the arm correspond to lower values of the mast flexural stiffness. A numerical investigation was performed to track the dependence of the structural natural frequency on the electrode elongation. This allowed drawing a map of the notch filter bandwidth versus the effective mast elongation, which is detected in real time mode by some position sensors (Figure 11).

## **9 Compact models and order reduction**

The above described FEM model is very detailed but too much expensive in terms of computational time for a straight implementation of a system control. It was developed to catch some typical phenomena due to a coupling effect among structural vibration, regulation command, electrical arc generation and scrap motion never clearly identified in the past. Nevertheless, it is evident that structural and control system designers need for a compact formulation to be used even in the time domain analysis of the dynamic response of the this plant. Two approaches were tested to simplify and reduce the number of degrees of freedom. A first attempt was performed by investigating the accuracy provided by a modelling based on beam elements (Figure 12).

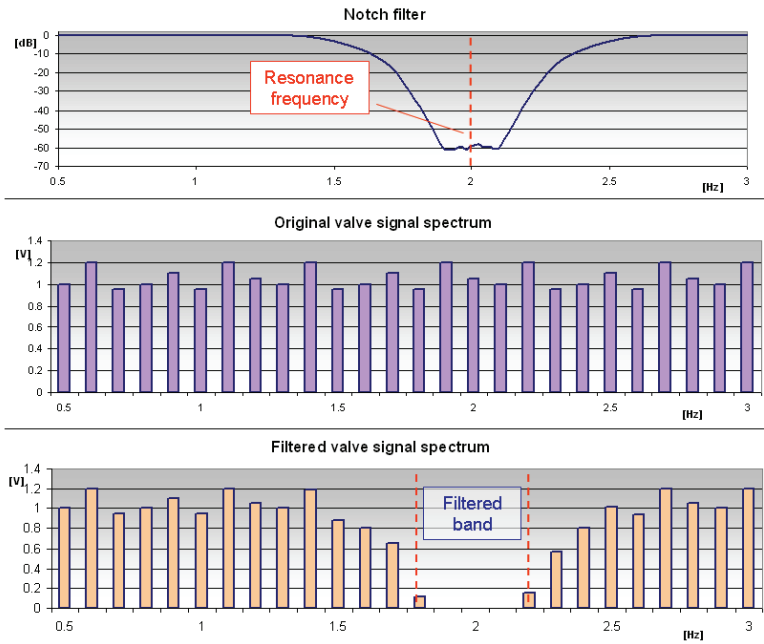


Figure 10: Notch filter and filtered valve position command

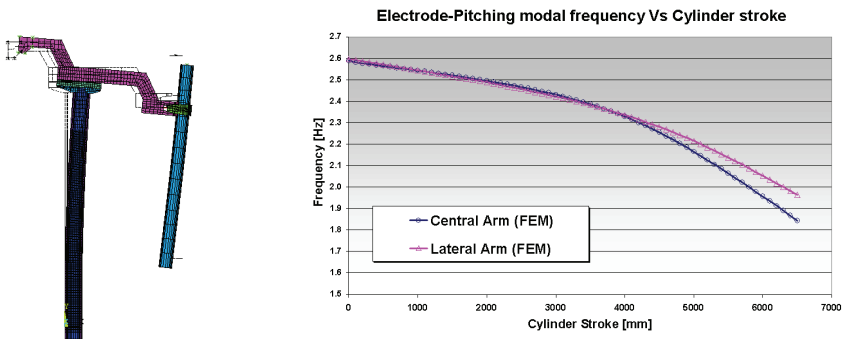


Figure 11: Electrode-pitching motion: modal frequency as function of the mast elevation

If only beam elements are used to model all the structural components results agree with experiments quite approximately, although FEM modelling is easier and solution is faster. In practice, effectiveness of this approach is insufficient for design activity. Therefore authors tested a different approach based on solid/shell elements

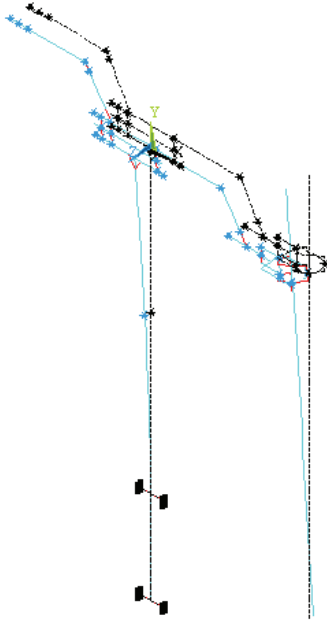


Figure 12: Lateral bending mode shape computed by the FEM beam-based model.

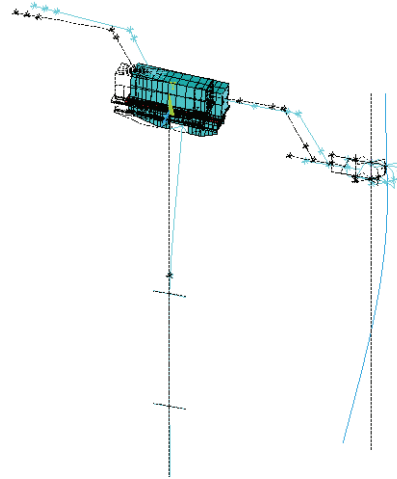


Figure 13: Mode shape F computed by the hybrid FEM beam/shell model

to model only the mast-to-arm connection and beam elements for column, arm and electrode respectively (Figure 13).

This approach allowed removing some assumptions made on the preliminary beam model, thus achieving an accurate prediction of the dynamic behaviour of the structure.

This simplification was judged sufficient for structural design, but the need for a simulation of the structural compliance and inertia within the electrode control system simulator required reducing further the degrees of freedom. This task was performed by exploiting the proved reliability of the solid/shell model to study the most important mode shapes, such as pitching and modes D and F, while using only a portion of the whole number of degrees of freedom. Two well known model order reduction techniques were considered. The so-called Modal Reduction introduced by Guyan [Guyan, 1965] and the Component Mode Synthesis (CMS) proposed by Craig and Bambpton [Craig and Bambpton, 1968] were implemented.

Guyan modal reduction suggests writing the equations of motion of the whole system by distinguishing the degrees of freedom to be retained in the reduced model

(so-called “Master DoFs”) from those which are condensed, being called “slave”. The inaccuracy introduced in dynamic analysis is larger as is the inertia associated to the slave DoFs [Genta, 1999]. This technique is shortly resumed in Appendix.

To assure the highest accuracy in the dynamic analysis, master DoFs were placed where inertial contribution is more relevant, mode shapes exhibit larger amplitudes and where sensors or actuators are applied. Modal analysis previously performed allowed selecting the most suitable master DoFs, in present case.

According to designer’s practice some typical degrees of freedom are enclosed into some lumped parameters models implemented to predict the EAF’s structural dynamics. To follow this usual approach only eleven nodes of the FEM model were tentatively chosen as master nodes. Translational degrees of freedom along X and Y axes associated to those nodes were retained as Master DoFs. No translation along Z direction was selected. This assumption evidently excludes torsional vibration modes and transversal bending shapes to focus only on the longitudinal flexural behaviour, acting within the structure’s symmetry plane. In addition, vertical motion was described by a DoF located onto the mast-to-cylinder connecting pin, to interface the resulting super-element and the regulation control action. In practice, connecting pin was supposed unconstrained and numerical results included the rigid body motion of the mast along the vertical direction.

This reduction led to have 23 Master DoFs (Figure 14-a) and allowed computing the first 23 non-transversal mode shapes of the structure. Table 4 shows a preliminary comparison between the numerical and experimental frequency values of the first 15 vibration modes. As it was meant to demonstrate, the limitation of the DoFs in the symmetry plane is losing the mode shapes in the perpendicular direction, even when the Guyan Reduction is used on a FEM model. Moreover, the 7<sup>th</sup> and 8<sup>th</sup> modes are poorly predicted, because to the coexistence of both longitudinal and transversal bending in the full model vibration shapes. Decreasing further the number of Master DoFs from 23 to 5 to replicate the information enclosed in some lumped parameter models currently used is possible. Only two structure monitoring points (Figure 14-b) may be selected as master, but the loss in the number of mode shapes calculated and in accuracy in predicting the higher frequency behaviour is fairly large.

The so-called Component Mode Synthesis (CMS) overcomes the accuracy limits of the Guyan’s method when reduction is forced to very few degrees of freedom. It allows distinguishing between the mode shapes of each substructure, usually referred to as “constrained modes”, and the dynamic response of few points used as interface with the other substructures. Actually this technique extracts the dynamic response of each substructure, in terms of mode shapes for a given condition of constraint, then applies its effects on the connections linking the main structure to

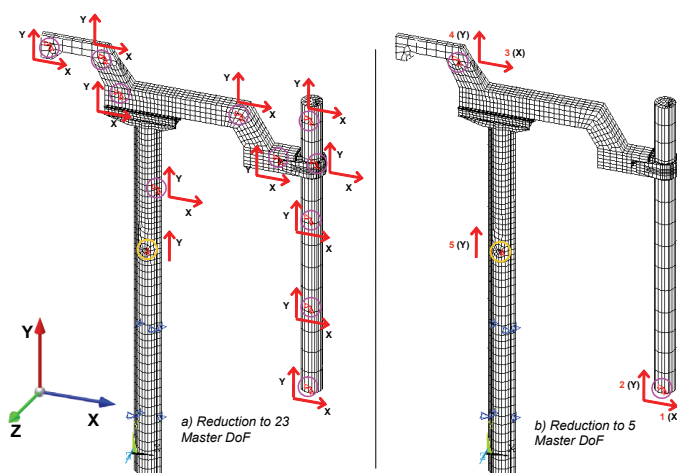


Figure 14: Master degrees of freedom of the solid/shell reduced model.

its components. In practice, the nodes of the substructures, so-called “internal”, correspond to the selection of the slave DoFs of Guyan’s formulation, while the “external or boundary” DoFs play the role of the master DoFs. External DoFs are those where loads, constraints and integrity conditions are applied. Some details are summarized in appendix.

The Craig-Bampton’s technique was applied to include 15 constrained mode shapes and the same 23 external DoFs used as masters in the previous described Guyan’s reduction. This reduction allowed predicting all the 15 mode shapes observed in Table 4, including transversal ones, thanks to the introduction of a good number of constrained modes. The accuracy reached was very good. A further reduction was tested on both the number of constrained modes and the number of external DoFs. Results of these tests are collected in Table 4.

A progressive loss in the number of predicted modes and in accuracy is observed as usual in reducing the dimension of the condensed matrices. The 23 master DoFs – 1 constrained mode CMS model gives results similar to those of the 23 DoFs Guyan, but allows higher accuracy in correspondence of the 7<sup>th</sup> and 8<sup>th</sup> eigenfrequencies. This result is due to the existence of a constrained mode representing the mode A of the full FEM solid/shell model. The 5 DoFs - 1 constrained mode CMS model gives the same accuracy of the 5 DoFs Guyan. No transversal bending was considered by results computed according to the Guyan’s method. Therefore the 2<sup>nd</sup> frequency, related to the constrained mode A, does not provide a useful definition to improve the accuracy of the longitudinal mode shapes’ eigenfrequencies. Both the 5-DoFs

Table 4: Comparison among the results of the reduced order and full models [Hz]

Mode	Displ. direction	Original FE model	Guyan				Craig-Bampton					
			23 DoF	Accur.	5 DoF	Accur.	23 DoF 15 Modes	Accur.	23 DoF 1 Mode	Accur.	5 DoF 1 Mode	Accur.
0	Y (free vertical motion)	0	0	100.0%	0	100.0%	0	100.0%	0	100.0%	0	100.0%
1	Transversal (Z)	1.8689	/	/	/	/	1.8689	100.0%	1.8694	100.0%	1.8689	100.0%
2	Transversal (Z)	2.0723	/	/	/	/	2.0723	100.0%	/	/	/	/
3	Longitudinal (XY)	2.3009	2.3012	100.0%	2.3052	99.8%	2.3011	100.0%	2.3012	100.0%	2.3052	99.8%
4	Longitudinal (XY)	2.8408	2.8415	100.0%	2.8709	98.9%	2.8015	98.6%	2.8415	100.0%	2.8709	98.9%
5	Transversal (Z)	4.1084	/	/	/	/	4.1084	100.0%	/	/	/	/
6	Longitudinal (XY)	6.9036	6.9093	99.9%	7.0588	97.8%	6.9116	99.9%	6.9095	99.9%	7.0591	97.7%
7	Mixed XY - Z	15.062	7.5722	50.3%	/	/	15.0618	100.0%	8.4631	56.2%	/	/
8	Mixed XY - Z	17.097	9.9036	57.9%	/	/	17.0969	100.0%	18.2824	93.1%	/	/
9	Longitudinal (XY)	18.561	18.8163	98.6%	28.7499	45.1%	18.8096	98.7%	18.8775	98.3%	28.7564	45.1%
10	Longitudinal (XY)	23.981	24.4936	97.9%	/	/	24.4705	98.0%	24.5577	97.6%	/	/
11	Transversal (Z)	28.675	/	/	/	/	28.675	100.0%	/	/	/	/
12	Transversal (Z)	31.138	/	/	/	/	31.1382	100.0%	/	/	/	/
13	Longitudinal (XY)	34.953	35.891	97.3%	/	/	35.8507	97.4%	35.8998	97.3%	/	/
14	Transversal (Z)	39.637	/	/	/	/	39.6393	100.0%	/	/	/	/
15	Longitudinal (XY)	41.178	45.5597	89.4%	/	/	42.1724	97.6%	45.7209	89.0%	/	/

reduced models provide an accuracy higher than 95% with respect to the validated full three dimensional model, at least below 7 Hz. Since the primary need of design at present consists in an effective control of the electrode pitching mode this accuracy demonstrated to be fitting the requirements of the customer. The Component Mode Synthesis appears more suitable for a compact modelling activity of the whole control system of the flexible structure. Better accuracy is easily achievable by simply increasing the number of the constrained modes included in the reduction operation. A sensitivity analysis on the value of the hydraulic cylinder stroke is described in Figure 15. A comparison with the results computed by the full FEM model is added for the most relevant mode shapes.

## 10 Perspectives of active vibration control

Future work will be focused on the active vibration control to be integrated with the process control action currently implemented for positioning the electrodes within the furnace. Presently the electrode regulation is operated by means of a constant impedance PID [Franklin et al., 1990]. It is aimed at raising or lowering the electrode structure to maintain the desired voltage and current. To avoid resonance a notch filter was applied to cut off the dangerous excitation due to the valve of the hydraulic actuator. Unfortunately, the structure is raising and lowering during the whole steelmaking process. Therefore the resonance frequency is continuously changing and the notch filter should be substituted by either an adaptive control or by applying a fairly large bandwidth in filtering [Franklin and Powell, 1990]. A slight improvement of the present study should be the correlation between the resonance frequency and the mast elevation to allow continuously resetting the notch filter with respect to the actual electrode position. A preferred development

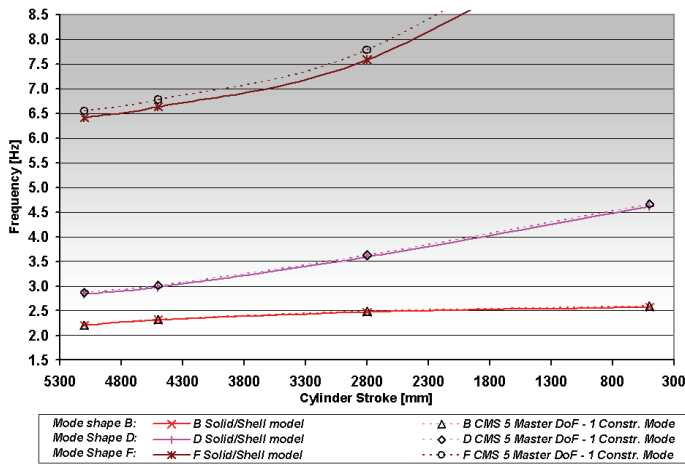


Figure 15: Comparison between the numerical results of the full and reduced FEM models and sensitivity on the cylinder stroke value for the most relevant mode shapes.

will be the design of an active control suitable for damping vibration according to [Meirovitch, 1999; Junkins and Kim, 1993]. This approach will resort to a modal control like it has been applied in active control systems developed for automotive suspension and robots [Da Silva et al., 2006] and even in civil structures subjected to seismic hazard [Pneumatikos and Gantes, 2005]. To reach this goal an addition is required. Since the structural mode cannot be directly accessed during operation, a real-time state observer is needed. The modal reduction approach previously described seems to be suitable to build up the observer by a state-space linear dynamic formulation, which could use few sensors. In principle, modal analysis suggests that a flight-time laser sensor precisely and rapidly gauging the distance to a target placed at the electrode arm tail should fit this requirement. Although this application has still to be tested in terms of accuracy and reliability, it was already proven by some preliminary tests that monitoring the pitching mode is possible by measuring the vertical displacement of the arm tail. This sensor gives three outputs: the electrode arm's position, the target's oscillation frequency and its speed. These data should allow interacting with the structure's regulator if two channels will be activated, i.e. a correction signal and a feedback. The first one will deserve as command for the cylinder regulation electro-valve, while the second, still to be defined, should give a reliable identification of the position of the structure.

Since the elevation of the EAF structure changes during the melting process, its

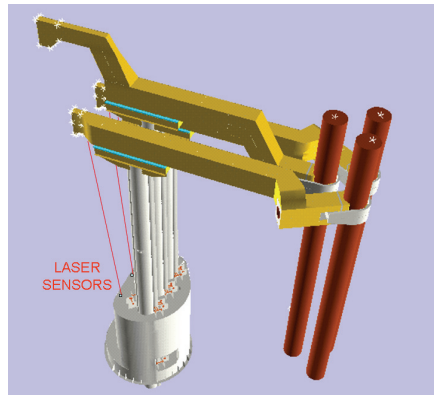


Figure 16: Laser sensors placement for vibration monitoring in operating conditions.

modal behaviour is subjected to continuous variations. To correct the state-space model, the system matrixes appearing within the equation of motion should be updated by performing a linear interpolation of their parameters, between a finite number of calculated position steps. This technique will follow the so-called Linear Parameter Varying Systems as proposed by Symens [Symens, 2004]. For a straight integration of the positioning and modal control a possible approach should be the application of fuzzy modal control tested by Malhis [Malhis, 2006]. Both these approaches need for the compact structural model above proposed.

## 11 Future actions

Main goal of the present work is the numerical prediction and prevention of undesired vibration in EAF's structure. Nevertheless, the occurring of some damages in operating condition may be suitably monitored through some dynamic approaches based on structural identification methods [Panda and Manohar, 2008; Venkatesha et al., 2008;] aimed at damage detection [Alaimo, 2008;] and even crack propagation monitoring [Zhang and Chen, 2008]. Implementation of compact models will be therefore useful in failure prevention. A next task of this research activity will be performed by screening the state of arts of identification methods applied to industrial structures like it was already preliminary done in [Daghia, 2008]. This action is required by industry, since EAF maintenance operation is expensive and rather difficult. Moreover, since damage monitoring may often involve nonlinearity, some further experiments will be completed to increase the computational performance of the proposed numerical model. In particular, two aspects will be verified. The

possibility of implementing non conventional numerical methods [Tonti and Zaran-tonello, 2009] to increase the fastness of the numerical solution will be investigated together with the capability of some approaches to improve the effectiveness of the compacting techniques [Hsin-Yi Lai et al., 2008; La Mantia and Dabnichki, 2008]. Authors will resort to a deeper thermomechanical analysis to investigate the coupling effect occurring in the electrodes during the EAF's operation. Coupled-field analysis will be implemented by following the successful approach already tested in the case of electromechanical coupling of microsystems and documented in [Bettini et al., 2008].

## **12 Conclusion**

Existing literature on Electric Arc Furnace points out that critical issues of design are the power control, failure prevention in structures and transformers, prediction of the energy and mass balances as well as of scrap and bath motion within the furnace. All those aspects are crucial for the process performance. They are strictly related to electrodes and structure vibration, although this topic does not appear yet in the specialized literature. The aim of this paper was identifying and modelling vibration effects in EAF to provide to control system designers an effective model of the dynamic behaviour of these compliant structures.

Some practical results were achieved. Electrode collision with ferrous scrap, causing severe short-circuits, is due not only to flexural modes shapes but evenly to torsional modes associated to the supporting arm, usually assumed to be perfect rigid bodies. Moreover, the maintenance audit set-up currently used for vibration monitoring appears neglecting some important measurement points, where sensors have to be located to detect even torsional modes. Detected instability of the electrical control variables and power supplying is due to irregularities in arc generation, being highly excited by differential flexural modes in which electrodes motion occurs in opposite directions. Common modes shapes, in which electrode structures move in the same direction, strongly affect the scrap motion within the furnace. Responsible of vibration mode excitation is even the regulation valve behaviour, which controls the electrode lifting. Cable mass connected to the electrodes, being usually neglected, has to be included in modelling to predict the actual resonance frequencies of the whole structure. Mode shapes occurring at the lowest frequencies are the most dangerous for the materials strength.

FEM models based on beam elements are quickly built up. They accurately predict only for the first three mode shapes (Figure 7: A, B and C), by introducing errors within 3 to 8 % with respect to the frequencies experimentally measured. Detailed FEM model based on shell elements look quite expensive in terms of computational time. They give a better agreement with the experimental results for all the

frequencies monitored. It was proven that a good compromise in terms of computational time and performance is assured by a sort of hybrid model, in which structure is modelled as beam elements, while the connection between arm and column is modelled by means of shells. A full three dimensional model including solid and shell elements gave the most detailed information to set up the regulator notch-filter, aimed at avoiding resonance during the melting process. This control was very recently tested on the working EAF plant. Results were very promising, since the average number of furnace heats between two subsequent electrode breakages was increased by 130%. Model reduction techniques were implemented to provide a compact model to the control system design. Craig Bambpton's approach appeared to be very effective in predicting all the relevant resonances, provided that the most important modes were introduced in the component mode synthesis. Compact model shall be successfully used to implement a modal control to be integrated with the hydraulic actuator regulation, which assures the electrodes lifting. A suitable feedback sensor is yet to be selected. Preliminary tests with laser sensors were performed. Few sensors may effectively point the tail of the supporting arm, although some problems related to the electrode conductive material have to be overcome.

**Acknowledgement:** Authors thank the Management and the Technical Staff of Sovel S.A. (Greece) for sharing the experimental results acquired during a maintenance audit and for contributing to the analysis of the structural behaviour of the monitored plant. In particular, among the above cited people, authors mention Eng. M. Ansoldi, Eng. F. Scotti, Mr. C. Nali, Eng. D. Alessio, all belonging Danieli Company – Italy, for their helpful contribution and suggestions. Authors are grateful to the Dept. Electrical, Management and Mechanical Engineering for supporting in Udine the computational activity performed in cooperation with R&D Dept. at Danieli and Politecnico di Torino.

## **References**

**Abraham, S.; Chen, S.** (2008): EAF energy and material balance modelling, *Iron and Steel Technology*, Special Issue on “Electric Steelmaking Technologies”, 5(2), pp.32-42.

**Alaimo A., Milazzo A.; Orlando C.** (2008): Global/local FEM-BEM stress analysis of damaged aircraft structures, *CMES: Computer Modeling in Engineering & Sciences*, 36(1), pp.23-41.

**ANSYS©** (2008): User's manual, vs.10.0/11.0, license 239588/2007/2008.

**Bermudez, A.; Bullon, J.; Pena, F.; Salgano, P.** (2003): A numerical method

for transient simulation of metallurgical compound electrodes, *Finite Elements in Analysis and Design*, 39, pp. 283–299.

**Bettini P.; Brusa E.; Munteanu M.; Specogna R.; Trevisan F. (2008):** Innovative Numerical Methods for nonlinear MEMS: the Non-Incremental FEM vs. the Discrete Geometric Approach, *CMES: Computer Modeling in Engineering & Sciences*, 33(3), pp.215-242.

**Bouganosopoulos, G.; Papantoniou, V.; Sismani, P. (2008):** Start-Up Experience and Results of Consteel@at the SOVEL Meltshop, *Iron and Steel Technology*, Special Issue on “Electric Steelmaking Technologies”, 9 (2), pp.38-46.

**Boyd, L.C.; Sikka, V.K. (2008):** Improving the system life of basic oxygen and electric arc furnace hoods, roofs and side vents, *Iron and Steel Technology*, Special Issue on “Electric Steelmaking Technologies”, 5 (2), pp.70-81.

**Camdali, U.; Tunc, M. (2003):** Exergy analysis and efficiency in an industrial AC electric ARC furnace, *Applied Thermal Engineering*, 23, pp.2255–2267.

**Chirattananon, S.; Gao, Z. (1996):** A model for the performance evaluation of the operation of electric arc furnace, *Energy Convers. Mgmt.*, 37(2), pp.161-166.

**Craig, R.R.Jr.; Bambpton, M.C.C. (1968):** Coupling of substructures for dynamic analysis, *AIAA Journal*, 6 (7), pp.1313-1319.

**Crompton, P. (2001):** The diffusion of new steelmaking technology, *Resources Policy*, 27, pp.87–95.

**Daghia F.; Hasan W.; Nobile L.; Viola E. (2008):** Parameter identification of beam-column structures on two-parameter elastic foundation, *CMES: Computer Modeling in Engineering & Sciences*, 39(1), pp.1-28,

**Da Silva, M.M.; Bröls, O.; Paijmans, B.; Desmet, W.; Van Brussel, H. (2006):** Concurrent Simulation of Mechatronic Systems with Variable Mechanical Configuration, *Proc. ISMA 2006 - AMSI - Multibody Dynamics for Multi-Physics Applications*.

**Dixon, G.F.L.; Kendall, P.G. (1972):** Supply to ARC Furnace: Measurement and Prediction of Supply-Voltage Fluctuation, *Proc. IEE* 119 (4), pp.456–465.

**Ekmekci, I.; Yetiskan, Y.; Camdali, U. (2007):** Mass balance modeling for Electric Arc Furnace and ladle furnace system in steelmaking facility in Turkey, *Iron and Steel Research*, 14(5), pp.01-06, sec.55.

**El-Saady, G. (2001):** Adaptive static VAR controller for simultaneous elimination of voltage flickers and phase current imbalances due to arc furnaces loads, *Electric Power Systems Research*, 58, pp.133–140.

**Ewins, D.J. (2000):** Modal testing: theory, practice and application, 2<sup>nd</sup> Edition, Research Studies Press Ltd. Baldock, England.

**Franceschinis, E.** (2007): Misura sperimentale, modelli numerici e algoritmo di controllo attivo delle vibrazioni di una struttura porta elettrodo per forno fusorio ad arco (“Experimental testing, numerical modelling and active vibration control of electrodes structure of EAF”), M.Sc. Degree thesis (in italian), University of Udine, Italy.

**Franklin, G.F.; Powell, J.D.** (1990): *Digital control systems*, Addison Wesley, Reading Massachussets.

**Franklin, G.F.; Powell, J.D.; Enami-Naeini, A.** (1990): *Feedback control of dynamic systems*, Addison Wesley, Reading Massachussets.

**Genta, G.** (1999): *Vibration of structures and machines*, Springer Verlag, New York, 3<sup>rd</sup> Edition.

**Guo, D. ; Irons, G.A.** (2007): Modelling of steel scrap movement, *Appl. Math. Modelling*, available on line as doi:10.1016/j.apm.2007.06.037.

**Guyan, R.J.** (1965): Reduction of stiffness and mass matrices, *AIAA Journal*, 3 (2), p.380-392.

**Hsin-Yi Lai; Chen C. K.; Jung-Chang Hsu** (2008): Free vibration of non-uniform Euler-Bernoulli beams by the Adomian Modified Decomposition Method, *CMES: Computer Modeling in Engineering & Sciences*, 34(1), pp.87-113.

**Inman, D.** (2008): *Vibration and control*, Prentice Hall, New York.

**Junkins, J.L.; Kim, Y.** (1993): *Introduction to dynamics and control of flexible structures*, AIAA publications, Washington.

**La Mantia M.; Dabnichki P.** (2008): Unsteady 3D Boundary Element Method for Oscillating Wing, *CMES: Computer Modeling in Engineering & Sciences*, 33(2), pp.131-153.

**Malhis, M.** (2006): Fuzzy modal active control of flexible structures, *Journal of Vibration and Control*, 11 (1), pp.67-88.

**Marsical, A.; Martinez, F.** (2008): Preventing EAF Transformer Failures, *Iron and Steel Technology*, Special Issue on “Electric Steelmaking Technologies”, 5(2), pp.49-56.

**Meirovitch, L.** (1999): *Dynamics and control of structures*, John Wiley and Sons, New York.

**Panda S.S.; Manohar C.S.** (2008) Applications of Meta-Models in Finite Element Based reliability Analysis of Engineering Structures, *CMES: Computer Modeling in Engineering & Sciences*, 28(3), pp.161-184.

**Pnevmatikos, N.G.; Gantes, C.J.** (2005): Design procedure for substructures equipped with a control system and subjected to earthquake loading, *Proc. 5<sup>th</sup>*

*GRACM International Congress on Computational Mechanics*, Limassol.

**Sandberg, E.; Lennox, B.; Undvall, P.** (2007): Scrap management by statistical evaluation of EAF process data, *Control Engineering Practice*, 15, pp.1063–1075

**Shinohara, A.; Goodall, D.P.** (2004): Robust set-point controllers for an electric arc furnace cooling system, *Control Engineering Practice*, 12, pp.799–810.

**Symens, W.** (2004): *Motion and Vibration Control of Mechatronic Systems with Variable Configuration and Local non-Linear Friction*, PhD Thesis, Katholieke Universiteit Leuven, Belgium.

**Tonti E.; Zarantonello F.** (2009): Algebraic formulation of elastostatics: the Cell Method, *CMES: Computer Modeling in Engineering & Sciences*, 39(3), pp.201-236.

**VDE - Verein Deutscher Eisenhüttenleute** (1992): *The Steel Manual*, translation of “Stahlfibel”, Verlag Stahleisen, Dusseldorf.

**Venkatesha S.; Rajender R.; Manohar C.S.** (2008): Inverse sensitivity analysis of singular solutions of FRF matrix in structural system identification, *CMES: Computer Modeling in Engineering & Sciences*, 37(2), pp.113-147.

**Wriggers, P.** (2006) *Computational contact mechanics*, Springer Verlag, Berlin and New York.

**Zhang Y.Y.; Chen L.** (2008): A simplified meshless method for dynamic crack growth, *CMES: Computer Modeling in Engineering & Sciences*, 31(3), pp.189-200.

## Appendix

### *Guyan's model order reduction*

The so-called Guyan's model order reduction applied to decrease the degrees of freedom of a discretized model distinguishes two sets of DoFs, being referred to as “master” and “slave”, respectively [Genta, 1999]. Equations of motion are therefore described as follows:

$$\begin{bmatrix} \mathbf{M}_{11} & \mathbf{M}_{12} \\ \mathbf{M}_{21} & \mathbf{M}_{22} \end{bmatrix} \begin{Bmatrix} \ddot{\mathbf{q}}_1 \\ \ddot{\mathbf{q}}_2 \end{Bmatrix} + \begin{bmatrix} \mathbf{C}_{11} & \mathbf{C}_{12} \\ \mathbf{C}_{21} & \mathbf{C}_{22} \end{bmatrix} \begin{Bmatrix} \dot{\mathbf{q}}_1 \\ \dot{\mathbf{q}}_2 \end{Bmatrix} + \begin{bmatrix} \mathbf{K}_{11} & \mathbf{K}_{12} \\ \mathbf{K}_{21} & \mathbf{K}_{22} \end{bmatrix} \begin{Bmatrix} \mathbf{q}_1 \\ \mathbf{q}_2 \end{Bmatrix} = \begin{Bmatrix} \mathbf{F}_1 \\ \mathbf{F}_2 \end{Bmatrix} \quad (\text{A1})$$

where  $\mathbf{q}_1$  and  $\mathbf{q}_2$  are the master and slave degrees of freedom, respectively.

The condensed matrices are [Genta, 1999] :

$$\begin{aligned}
 \mathbf{K}_{cond} &= \mathbf{K}_{11} - \mathbf{K}_{12} \mathbf{K}_{22}^{-1} \mathbf{K}_{12}^T \\
 \mathbf{F}_{cond} &= \mathbf{F}_1 - \mathbf{K}_{12} \mathbf{K}_{22}^{-1} \mathbf{F}_2 \\
 \mathbf{M}_{cond} &= \mathbf{M}_{11} - \mathbf{M}_{12} \mathbf{K}_{22}^{-1} \mathbf{K}_{12}^T \\
 &\quad - (\mathbf{M}_{12} \mathbf{K}_{22}^{-1} \mathbf{K}_{12}^T)^T + \mathbf{K}_{12} \mathbf{K}_{22}^{-1} \mathbf{M}_{22} \mathbf{K}_{22}^{-1} \mathbf{K}_{12}^T \\
 \mathbf{C}_{cond} &= \mathbf{C}_{11} - \mathbf{C}_{12} \mathbf{K}_{22}^{-1} \mathbf{K}_{12}^T \\
 &\quad - (\mathbf{C}_{12} \mathbf{K}_{22}^{-1} \mathbf{K}_{12}^T)^T + \mathbf{K}_{12} \mathbf{K}_{22}^{-1} \mathbf{C}_{22} \mathbf{K}_{22}^{-1} \mathbf{K}_{12}^T
 \end{aligned} \tag{A2}$$

The inertial contribution of the slave DoFs, namely  $\mathbf{M}_{21}$ , is neglected. This assumption may introduce some approximation in the reduced model [Genta, 1999]. Slave DoFs do not explicitly appear in the condensed equation of motion:

$$\mathbf{M}_{cond} \ddot{\mathbf{q}}_1 + \mathbf{C}_{cond} \dot{\mathbf{q}}_1 + \mathbf{K}_{cond} \mathbf{q}_1 = \mathbf{F}_1 \tag{A3}$$

This formulation allows reducing the computational effort in solution. Eigenvalues and eigenvectors are extracted from Eq.(A.3) thus computing the related natural frequencies and vibration mode shapes of the system. Master DoFs are first computed, then slave DoFs are easily derived.

### *Craig-Bambpton's component mode synthesis*

Craig and Bambpton suggested a different approach [Craig and Bambpton, 1968]. It is aimed at enhancing the performance of the solution algorithm, particularly where mechanical systems can be substructured. A structure is seen as the assembly of subsystems, each one interpreted as super-element. This assumption allows defining few nodes connecting the super element to the whole structure. Several nodes and elements are used to describe the behaviour of the super-element, seen as a stand-alone structure, being then connected and constrained to the main frame. This operation allows distinguishing between an internal and external domain respectively.

A first eigenproblem is solved for the internal DoFs, corresponding to the nodes of the substructure, by assuming that the boundary nodes, where substructure and main frame are connected, are fixed. The substructure's normal eigenvectors  $\Phi^I$  are computed and arranged in the matrix  $\Phi^N$  which includes the constrained modes:

$$\omega^2 \cdot \mathbf{M}_{II} \cdot \Phi^I = \mathbf{K}_{II} \cdot \Phi^I \tag{A4}$$

$$\Phi^N = (\Phi^I)_{1, \dots, n}$$

Displacements are then expressed as linear combination of the constrained modes of the substructure and of the boundary modes, by means of the transformation matrix  $\alpha$ :

$$\alpha = \begin{pmatrix} \mathbf{I} & \mathbf{0} \\ \Phi^B & \Phi^{CB} \end{pmatrix} \quad (\text{A5})$$

where  $\Phi^B$  is the matrix of the boundary DoFs' mode shapes and  $\Phi^{CB}$  is the Craig-Bambpton's base. The latter contains a selected number of the sub-structure's constrained modes, assumed to be significant for the analysis. The reduced problem is formulated as follows:

$$\alpha^T \cdot \mathbf{M} \cdot \alpha \cdot \frac{d^2}{dt^2} \mathbf{p} + \alpha^T \cdot \mathbf{K} \cdot \alpha \cdot \mathbf{p} = 0 \quad (\text{A6})$$

$$\mathbf{M}^{CB} \cdot \frac{d^2}{dt^2} \mathbf{p} + \mathbf{K}^{CB} \cdot \mathbf{p} = 0 \quad (\text{A7})$$

It is described as a function of the generalised coordinates:

$$\mathbf{p} = \begin{pmatrix} \mathbf{q}_B \\ \mathbf{p}^N \end{pmatrix} \quad (\text{A8})$$

where  $\mathbf{q}_B$  are the boundary nodes' displacements and  $\mathbf{p}^N$  are the normal mode shapes' amplitudes in the Craig-Bambpton's base.

The hypothesis of the Craig-Bambpton method lead to a stiffness matrix [Craig and Bambpton, 1968]:

$$\mathbf{K}^{CB} = \begin{pmatrix} \mathbf{K}^{BB} & \mathbf{0} \\ \mathbf{0} & \mathbf{K}^{NN} \end{pmatrix} \quad (\text{A9})$$

Matrix structure is banded diagonal, as long as the boundary nodes' contribution to the constrained mode shapes' amplitude are defined null, and diagonal for the partition corresponding to:

$$\mathbf{K}^{NN} = \Phi^{CB^T} \cdot \mathbf{K}_I \cdot \Phi^{CB} \quad (\text{A10})$$

The mass matrix is sparse:

$$\mathbf{M}^{CB} = \begin{pmatrix} \mathbf{M}^{BB} & \mathbf{M}^{BN} \\ \mathbf{M}^{BN^T} & \mathbf{M}^{NN} \end{pmatrix} \quad (\text{A11})$$

while the partition

$$\mathbf{M}^{NN} = \Phi^{CB^T} \cdot \mathbf{M}_I \cdot \Phi^{CB} \quad (\text{A12})$$

is diagonal, being orthogonal the sub-structure's normal mode shapes.

Accuracy of the solution of the reduced order problem depends on the selection of the Master DoFs and the number of the retained constraint mode shapes.